# Design Considerations for the Tooth Shoe Shape for High-Speed Permanent Magnet Generators

He Zhang[1,3], Xiaochen Zhang[2,3], Chris Gerada[1,3], Michael Galea[3], David Gerada[4], and Jing Li[3]

[1]The University of Nottingham, Ningbo 315100, China
[2]School of Electrical Engineering, Beijing Jiaotong University, Beijing 100044, China
[3]The University of Nottingham, Nottingham NG7 2RD, U.K.
[4]Cummins Generator Technologies, Stamford PE9 2NB, U.K.

**This paper presents a study of the effects that the shoe shape of the teeth of electrical machines has on the performance and losses. This is done by considering a concentrated wound, high-speed permanent magnet generator. The paper investigates the influence of the tooth shoe shape on the machine magnetic circuit and the losses distribution based on analytical and finite-element analysis (FEA). A shape coefficient $K_t$ is proposed to provide an optimized design reference. A comprehensive analytical tool able to study the variations of the machine performance parameters is proposed. The deduced optimization function is normalized using the non-equilibrium relative weighting method, and then, it is processed via a genetic algorithm to achieve the optimized design. FEA is used to validate the proposed analytical tool and the optimum design.**

***Index Terms*— Electromagnetic, genetic algorithm (GA), high-speed electrical machine, optimization, tooth shoe.**

## I. Introduction

NOWADAYS, there is increasing attention being paid to the development of high-speed machines, including motors and generators. In particular, permanent magnet (PM) machines are gaining more interest due to their outstanding efficiency, high power density, simple mechanical construction, and high reliability. The higher the motor speed, the smaller the electric machine volume for the same power output. However, the thermal or loss density of the machine is proportional to its power density, and the structure design aiming to have better loss distribution becomes a practical challenge for high-speed machines [1]–[3].

A metal sleeve is normally used to retain the magnets on a rotor outer surface, which can potentially result in large eddy losses for machines operating with a very high frequency. In most cases, there is no specified cooling strategy for the rotor, and thus the generated eddy loss may increase the rotor operating temperature to its thermal limit, which poses threats, such as partial demagnetization, for the PMs and to the stable operation of the machine. Therefore, the design of high-speed electrical machine needs to consider all the interactions among the electromagnetic, mechanical, and thermal aspects.

There is a wealth of literature looking into minimizing eddy-current losses in the rotor sleeve. In general, this is mainly focused on determining and minimizing eddy-current losses while still providing mechanical integrity, which may benefit both the machine efficiency and the thermal management. This is usually done by focusing on the electromagnetic field calculation and loss analyses. The influence of the slot shape on the eddy loss is considered in [4]. Another approach is to implement a high-performance thermal strategy [5], while optimization the design of high-speed electric machines is shown in [6].

Manuscript received March 20, 2015; revised May 16, 2015; accepted June 15, 2015. Corresponding author: X. Zhang (e-mail: xchzhang@bjtu.edu.cn).

Color versions of one or more of the figures in this paper are available online at http://ieeexplore.ieee.org.

Digital Object Identifier 10.1109/TMAG.2015.2448096

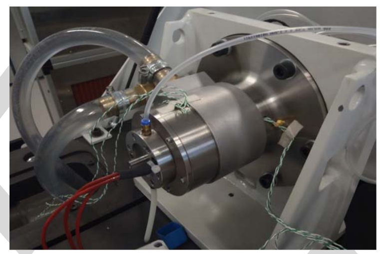

Fig. 1. Prototype of high-speed PM generator.

In this paper, a 3 kW, 80 000 r/min high-speed PM generator is investigated. Its stator tooth shoe shape is optimized, in order to reduce the eddy losses in the rotor sleeve and the rotor working temperature. Other performance parameters, such as efficiency and harmonics, are also included in the optimization process.

## II. FEA on a High-Speed Machine

The generator studied in this paper is fitted with a water jacket on the stator. In order to reduce the machine total length and increase the effective cooling area, the machine has concentrated windings. The rated output power is 3 kW at a rated speed of 80 000 r/min.

The rotor is excited by the PMs, which are retained by a sleeve, which is made of titanium alloy with a resistivity of $1.78 \times 10^{-6}$ Ω/m. The PM material is NdFeB35, with a magnetic remanence of 1.1 T, magnetic coercivity of $890 \times 10^3$ A/m, and maximum working temperature of 180 °C. For the stator core, where the losses are related to the steel laminations (grade and weight) and the alternating frequency of magnetic field, it is important to use high-frequency electrical steel for the high-speed machines. In this case, silicon steel with a thickness of 0.1 mm is used for the stator core. The manufactured prototype is shown in Fig. 1.

The field-circuit coupling analysis method is adopted in order to simplify the analytical modeling and to maintain a good accuracy. The stator end windings resistance and end windings leakage reactance are considered by adding

AQ:3

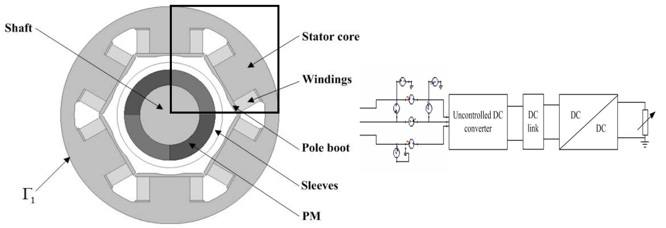


Fig. 2. System-level electromagnetic analysis model.

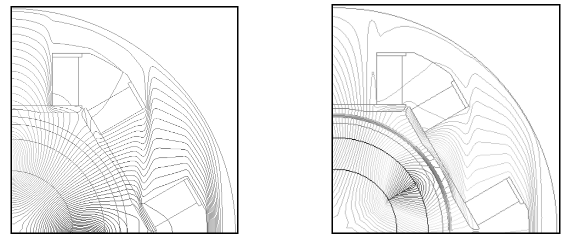

(a) (b)

Fig. 3. Loaded and no-load flux distribution in CW high-speed machines. (a) No load. (b) Under load. AQ:7

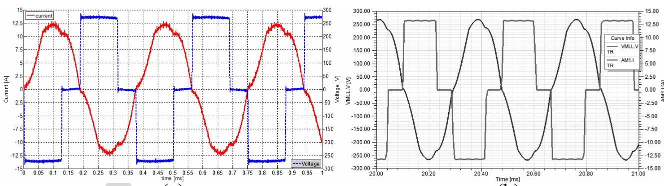

(a) (b)

Fig. 4. Comparisons of (a) measured and (b) calculated voltage and current.

TABLE I
COMPARISON OF CALCULATED RESULTS WITH TEST DATA OF HSPGS WITH OR WITHOUT PCS

| Speed (krpm) | | | measured | calculated | error |
|---|---|---|---|---|---|
| Without PCS | 70 | Line-Line Voltage (V) | 238.2 | 235.3 | -1.22% |
| | | Phase Current (A) | 2.4 | 2.36 | -1.67% |
| | 80 | Line-Line Voltage (V) | 242.7 | 237.5 | -2.14% |
| | | Phase Current (A) | 7.2 | 7.02 | -2.50% |
| With PCS | 70 | DC Voltage (V) | 16.2 | 15.8 | -2.47% |
| | | DC Current (A) | 49.5 | 48.4 | -2.22% |
| | 80 | DC Voltage (V) | 29.5 | 28.7 | -2.71% |
| | | DC Current (A) | 93.5 | 91.1 | -2.57% |

a resistance and an inductance in the power circuit. However, the model does not consider the 3-D eddy-current distribution, and thus, the eddy-current loss in the sleeve outside the core length region is neglected. The stator windings are set to be stranded coils. AQ:4 Considering that the diameter of the strands of the paralleled wire is very small, the displacement current and the Kelvin effect in the stator core and windings are ignored in this calculation [1]. In addition, because the machine is operating as a generator and the input torque is very small (0.43 N $\cdot$ m at 80k r/min), the cogging torque and vibration are to be ignored in the analytical and the experimental studies.

Based on the assumptions above, the 2-D cross section of the machine, as shown in Fig. 2, is used to develop the analytical model. The transient mathematical model for the 2-D electromagnetic field calculation is given in (1), where $\Omega$ is the calculation region, $A_z$ and $J_z$ are the magnetic vector potential and the source current density in the $z$-axial component, $J_s$ is the equivalent face current density of PM, and $\sigma$ is conductivity. $\Gamma_1$ is the parallel boundary condition, $\Gamma_2$ is the PM-region boundary condition, $\mu_1$ and $\mu_2$ are the relative permeability of the two different regions, and $n$ is the normal direction of PM-region boundary

$$\begin{cases}\Omega\colon \dfrac{\partial}{\partial x}\left(\dfrac{1}{\mu}\dfrac{\partial A_z}{\partial x}\right)+\dfrac{\partial}{\partial y}\left(\dfrac{1}{\mu}\dfrac{\partial A_z}{\partial y}\right)=-\left(J_z-\sigma\dfrac{dA_z}{dt}\right)\\ \Gamma_1\colon A_z=0\\ \Gamma_2\colon \dfrac{1}{\mu_1}\dfrac{\partial A_z}{\partial n}-\dfrac{1}{\mu_2}\dfrac{\partial A_z}{\partial n}=J_s.\end{cases} \tag{1}$$

AQ:5 To investigate the influence of power converter system (PCS) on machine performance, a direct coupled system level model is established, based on the proposed 2-D model, in which the 2-D finite-element analysis (FEA) to a PCS, which includes the uncontrolled rectifier, the dc–dc converter, the dc link filter, and the equivalent load resistance. The switching frequency of the device is 20 kHz, the gain of the dc–dc converter is 0.3, and the modulation radio is 15. The equivalent load resistance is 0.32 $\Omega$. AQ:6

From the co-simulation with the PCS, flux distributions of machine are obtained, and the flux distribution and air-gap flux density are shown in Fig. 3, in which the detail distributions in one-quarter of the calculation model (within the box in Fig. 2) are outlined. The magnetic field varies under load condition compared with no-load condition due to the stator armature reaction field, and flux density becomes lower and is distributed more asymmetrically, introducing more harmonics. The magnetic density within the stator core area is obtained from the analytical modeling. The transient variation of core loss is obtained via summing all the elements core loss.

From the analysis above, the time-varying cycle $T_e$ of the eddy-current density in each element is obtained, and the eddy loss in the sleeve caused by the stator windings armature magnetomotive force (MMF) and tooth harmonic MMF can be determined [4]. The friction losses of the rotor at different speeds are determined by the method mentioned in [7]. For the rated operation, the rotor friction loss is calculated as 12.9 W.

Fig. 4 shows the comparisons of the phase current and the line-to-line voltage of the high-speed generator operating under 80k r/min and 3 kW output between the experimental results and the simulated curves. In the time domain, the simulation results show good agreement with the measured ones. The experimental results have much more high-frequency harmonics than the simulation due to the operation of the rectifier and the dc–dc converter. The calculated current amplitude is ~6%, higher than the test value, and there is 3% difference in the voltage, respectively.

Table I shows the variations of the machine output terminal voltage and the current with and without PCS. When with the PCS, the 238 V ac line-to-line voltage is converted to 16.2 V dc voltage, and the 2.4 A phase current ac current is converted to 49.5 A dc current while generator operating under 70k r/min. In this test, the input of the generator is 0.185 N $\cdot$ m, and it was measured that the efficiency of machine reduces from 71.8% to 71.4% after the implementation of the PCs; the efficiency of the generator is only 59.1%. Whereas for operating under a speed of 80k r/min, the system efficiency is reduced $\sim$11%.

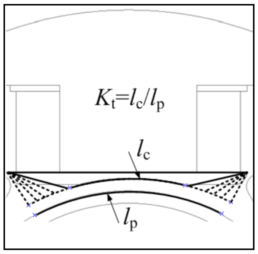


Fig. 5. Tooth shoe shape coefficient $K_t$ definition.

TABLE II
PERFORMANCE OF MACHINE WITH DIFFERENT TOOTH TOP (WITHOUT PCS)

| $l_c$ (mm) | $K_t$ | Phase voltage V | Phase current A | Output power W | Pcore W | Peddy W | Efficiency % |
|---|---|---|---|---|---|---|---|
| 16.82 | 0.97 | 106.87 | 5.35 | 1715.21 | 59.50 | 38.90 | 0.72 |
| 16.49 | 0.95 | 112.91 | 5.68 | 1923.99 | 62.04 | 42.64 | 0.74 |
| 16.09 | 0.93 | 118.48 | 5.96 | 2118.42 | 62.63 | 46.42 | 0.76 |
| 15.59 | 0.90 | 124.04 | 6.23 | 2318.37 | 64.33 | 49.67 | 0.77 |
| 14.94 | 0.86 | 129.17 | 6.46 | 2503.38 | 66.68 | 54.00 | 0.79 |
| 13.49 | 0.78 | 137.92 | 6.91 | 2859.01 | 69.47 | 55.67 | 0.81 |
| 10.64 | 0.62 | 150.00 | 7.50 | 3375.00 | 73.50 | 58.50 | 0.83 |
| 5.37 | 0.31 | 162.81 | 8.15 | 3980.62 | 75.80 | 71.95 | 0.85 |

## III. OPTIMIZATION OF STATOR TOOTH SHOE SHAPE

The shape of the stator tooth shoe not only affects the machine main magnetic circuit, but also has influences on the tooth spatial harmonics. This becomes more important in a high-speed machine with concentrated windings [3], [4]. A concentrated winding with one stator pole pitch is designed for the machine. In order to quantify the optimization and design effort, a shape coefficient $K_t$ is proposed and is defined as the ratio of the stator tooth top pitch length $l_c$ to the pole pitch length $l_p$. $K_t$ in the original design is 0.67. Fig. 5 shows the tooth shoe shape coefficient definition.

The variations of the machine terminal voltage, the armature current, the stator iron loss, the rotor eddy loss, and the machine efficiency are calculated via the FEA analysis. The variations of the machine performance with the stator tooth top length are listed in Table II. It can be observed how for a decreasing of tooth top pitch, the phase terminal voltage, the phase current, and the machine output power are increasing gradually. However, the stator core loss increases notably because of the incensement of main flux, as shown in Figs. 6 and 7. For the increase of harmonics, rotor eddy loss is also increased.

In order to further optimize the machine performance in terms of voltage, losses, and efficiency, a genetic algorithm (GA) is applied for the design progress. Based on the detail performance parameters variations obtained previously, using high-order polynomial analytic function fitting (fitting accuracy is larger than 0.9992), the proposed optimization functions are listed

$$\begin{cases} f_u(K_t) = 224.6 - 347.6 \times K_t + 593.5 \times K_t^2 - 369.1 \times K_t^3 \\ f_i(K_t) = 11.36 - 18.02 \times K_t + 30.63 \times K_t^2 - 18.83 \times K_t^3 \\ f_{\mathrm{pi}}(K_t) = 83.5 - 47.51 \times K_t + 96.33 \times K_t^2 - 74.33 \times K_t^3 \\ f_{\mathrm{pe}}(K_t) = 177.9 - 585.5 \times K_t + 943.3 \times K_t^2 - 501.1 \times K_t^3 \\ f_{\mathrm{eff}}(K_t) = 1.047 - 0.8921 \times K_t + 1.607 \times K_t^2 - 0.9656 \times K_t^3 \end{cases} \tag{2}$$

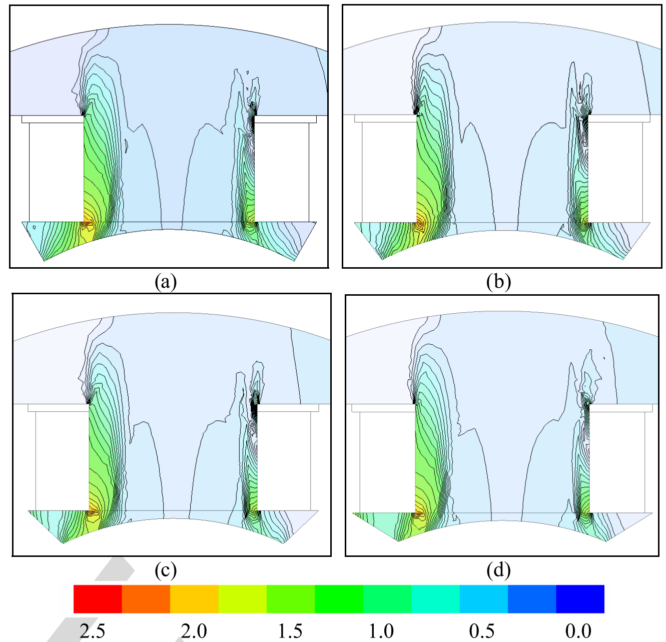


Fig. 6. Flux density distributions in machine with different values of $K_t$. (a) $K_t = 0.97$. (b) $K_t = 0.93$. (c) $K_t = 0.86$. (d) $K_t = 0.62$.

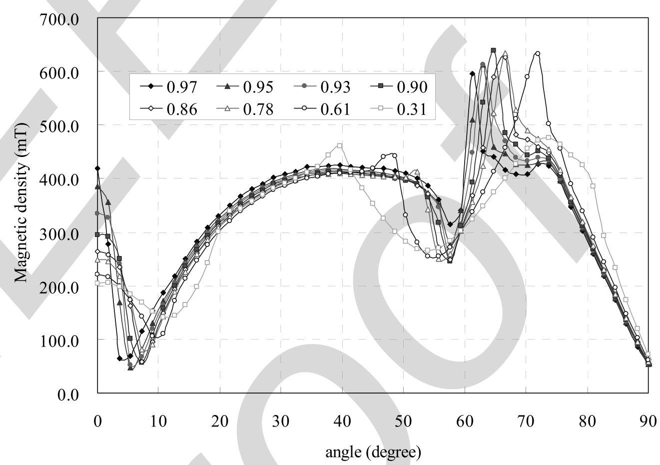


Fig. 7. Magnetic density in air gap of machine with different values of $K_t$ (one pole).

where $f_u(K_t)$ is the function of the stator terminal voltage (in volt); $f_i(K_t)$ is the function of armature current (in ampere); $f_{\mathrm{pi}}(K_t)$ is the function of stator iron loss (in watt); $f_{\mathrm{pe}}(K_t)$ is the function of rotor eddy loss (in watt); $f_{\mathrm{eff}}(K_t)$ is the function of generator efficiency (in percentage); and $0 < K_t < 1$.

The boundary condition, such as the terminal voltage, output power, and so on, is set up for the optimization. Therefore, the values of unequal weighting coefficient $\omega$ are adopted in the objective function establishment. Meanwhile, to avoid the influences of the numerical size differences among machine different performance physical parameters, a relative parameter optimization method is introduced.

Integrating the electromagnetic performance objectives, a combined optimization model on tooth shoe shape aim at electromagnetic and thermal performances is proposed, which could be written as

$$\max F'(K_t) = \omega \cdot Bs_N^T \cdot F(K_t)^T \tag{3}$$

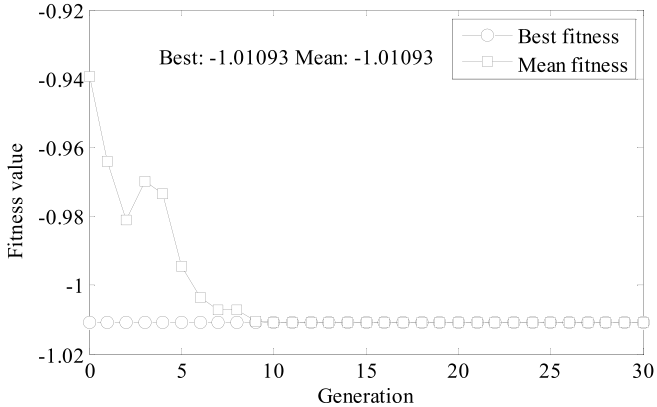


Fig. 8. Curves of fitness in GA iteration process.

where $\omega = [\omega_1, \omega_2, \omega_3, \omega_4, \omega_5]$

$$Bs_N = \left[\frac{1}{U_N}, \frac{1}{I_N}, \frac{1}{P_{\text{score}}}, \frac{1}{P_{\text{eddy}}}, \frac{1}{\text{Eff}i}\right]$$

$$F(K_t) = [f_u(K_t), f_i(K_t), f_{\text{pi}}(K_t), f_{\text{pe}}(K_t), f_{\text{eff}}(K_t)]$$

where $U_N$ is the rated voltage, $I_N$ is the rated current, and $P_{\text{eddy}}$ and $P_{\text{score}}$ are the rotor eddy loss and the stator core loss of high-speed machine under rated condition, respectively.

Constraint conditions are $F(K_t) > 0$ and $0 < K_t < 1$.

Using the GA [7], the objective function is processed solved. A fitness function (4) is established according to the GA and the objective function

$$\text{Fit}(K_t) = -\max F'(K_t) \tag{4}$$

where $0 < K_t \leq 1$.

In the GA optimizing process, after preliminary design, the initial population $m = 50$ is defined, and the evolution generation is 50. The scattered disorder data cross method (probability = 0.55), the Gaussian mutation strategy (probability = 0.05), and the former direction migration patterns are adopted. After several iterative calculations, the minimum value of the fitness function could be obtained, which is also the desired maximum value of the objective function within the constraint region. When the weighting coefficient $\omega$ is [0.55, 0.4, −0.1, −0.4, and 0.55], the variation curves of both the optimal fitness value and the average fitness value are shown in Fig. 8. At the 12th iteration, such two fitness values are −1.0109 and −1.01093, respectively. Thus, the optimal value of the objective function could be considered as 1.0109, and the corresponding variable $K_t$ is 0.4705.

To verify the obtained results, the electromagnetic performance of the high-speed machine with the optimized tooth shoe shape is analyzed via the FEA on the transient electromagnetic field calculation. The obtained performance parameters from the two methods are listed in Table III, in which the objective parameters determined by the GA agree with those obtained from numerical analyses.

The high-speed PM generator studied in this paper is with a power level of 3 kW, with the design requirements of operating power region within 8%, and the allowed machine line voltage change is within 5%. Using the optimized stator tooth top pitch of 8.13 mm, as shown in Table III, the phase terminal voltage is 143.07 V and the output power is 3.07 kW, which still satisfy the requirements. The efficiency of the machine increases from 86% to 87%. On the other hand, the increase of stator core loss and rotor eddy loss is controlled by the weighting coefficients. Thus, the optimized tooth shoe could promote a better performance of high-speed PM generator.

TABLE III
COMPARISONS OF OPTIMIZED AND NUMERICAL CALCULATED PARAMETERS

| | Numerical Calculated | GA Optimized | Error |
|---|---|---|---|
| Machine line voltage (V) | 143.07 | 147.99 | +3.44% |
| Armature current (A) | 7.16 | 7.40 | +3.27% |
| Output power (W) | 3073.79 | 3283.49 | +6.82% |
| Stator iron loss(W) | 74.60 | 74.73 | +0.18% |
| Rotor eddy loss(W) | 56.88 | 59.05 | +3.82% |
| Efficiency (%) | 0.8409 | 0.8424 | +0.18% |

## IV. CONCLUSION

From the comparison of the obtained results from different methods, it can be concluded that the optimized tooth shoe shape could improve the operating performance of the high-speed PM machines, especially for efficiency, eddy-current losses in metal sleeve, and the reduction in harmonics. However, the actual application of such a shape would be limited by the machine size and the manufactured processing technologies. Thus, such related factors will be studied and included in the further research work.

## ACKNOWLEDGMENT

This work was supported in part by the Ningbo Science and Technology Bureau in China under Grant 2014D10013 and in part by the National Natural Science Foundation of China under Grant 51407006.

## REFERENCES

[1] D.-K. Hong, B.-C. Woo, J.-Y. Lee, and D.-H. Koo, "Ultra high speed motor supported by air foil bearings for air blower cooling fuel cells," *IEEE Trans. Magn.*, vol. 48, no. 2, pp. 871–874, Feb. 2012. AQ:9

[2] D. Gerada *et al.*, "Design aspects of high-speed high-power-density laminated-rotor induction machines," *IEEE Trans. Ind. Electron.*, vol. 58, no. 9, pp. 4039–4047, Sep. 2011.

[3] J. Fang, X. Liu, B. Han, and K. Wang, "Analysis of circulating current loss for high-speed permanent magnet motor," *IEEE Trans. Magn.*, vol. 51, no. 1, Jan. 2015, Art. ID 8200113.

[4] X. Zhang *et al.*, "Electrothermal combined optimization on notch in air-cooled high-speed permanent-magnet generator," *IEEE Trans. Magn.*, vol. 51, no. 1, Jan. 2015, Art. ID 8200210.

[5] J. Zhang *et al.*, "Evaluation of applying retaining shield rotor for high-speed interior permanent magnet motors," *IEEE Trans. Magn.*, vol. 51, no. 3, Mar. 2015, Art. ID 8100404.

[6] C. C. Hwang, S. S. Hung, C. T. Liu, and S. P. Cheng, "Optimal design of a high speed SPM motor for machine tool applications," *IEEE Trans. Magn.*, vol. 50, no. 1, Jan. 2014, Art. ID 4002304.

[7] L. Weili, Z. Xiaochen, C. Shukang, and C. Junci, "Thermal optimization for a HSPMG used for distributed generation systems," *IEEE Trans. Ind. Electron.*, vol. 60, no. 2, pp. 474–482, Feb. 2013.